IEEE Access
Multidisciplinary | Rapid Review | Open Access Journal

SPECIAL SECTION ON ADVANCED CONTROL AND HEALTH MANAGEMENT FOR AIRCRAFT AND ITS PROPULSION SYSTEM

Received July 30, 2017, accepted August 16, 2017, date of publication August 29, 2017, date of current version September 19, 2017.

*Digital Object Identifier 10.1109/ACCESS.2017.2745701*

# Finite Time Fault Tolerant Attitude Control-Based Observer for a Rigid Satellite Subject to Thruster Faults

**A. AIHUA ZHANG, (Member, IEEE), B. CHENGCONG LV, C. ZHIQIANG ZHANG, AND D. ZHIYONG SHE**

College of Engineering, Bohai University, Jinzhou 121013, China

Corresponding author: A. Aihua Zhang (jsxinxi_zah@163.com)

This work was supported in part by the National Natural Science Foundation of China under Project 61603056, in part by the National Natural Science Foundation of Liaoning under Project 2015020042, and in part by the Excellent Talents to Support Projects in Liaoning Province of China under Project LJQ2015003.

**ABSTRACT** A rigid satellite fault diagnosis strategy, subject to faults of external disturbances and thruster faults, is developed. In this design, an equivalent idea is introduced to design a sliding mode observer that can detect and identify the failures indicated previously. Considering the measurability of parameters of the satellite, such as angular velocity and attitude, a sliding mode observer is implemented. Next, the amplitudes of the faults and disturbances can be detected, identified, and estimated via the sliding mode observer; these tasks are accomplished with zero estimation error within a finite period. A sliding mode-based attitude controller is developed using an exponential reaching law that relies on the system states and the corresponding formation of the estimated parameters. The controller not only guarantees the attitude system to be stable but also governs the attitude and angular velocity to converge to zero within a finite period. The good reliability of the proposed controller can be proved via multiple simulation tests.

**INDEX TERMS** Fault diagnosis, fault tolerant control, fault estimation, finite-time control.

## I. INTRODUCTION

Fault diagnosis (FD) and fault tolerance control (FTC) methods are consistently popular topics in engineering application fields. Zhiwei Gao et al. provided a summary of the fruitful FD and FTC methods and presented their use in different engineering applications fields in recent research papers [1], [2]. In similar research works, Sliding Mode Control (SMC) is indispensable. More in-depth discussion on how to use SMC technology in control field had been studied deeply in the past [3] . The controller developed by using SMC has great robustness to uncertainty, whether modeling uncertainties or external disturbances. For example, in Shen Yin as well as [4] and [5] of others, whatever for Markovian Jump Systems or switched systems, the stabilization problem for the system with output disturbances, actuator and sensor faults simultaneously are all considered. The uncertainty information can be obtained via an observer, and then the FTC will be done based the observer. For an SMC system design, two design sections, such as sliding surface and controller based SMC (SMCC), are necessary. The system states should reach the sliding surface using SMCC, that is, the expected convergence property can be ensured in the sliding surface [6], [7]. As a result, the good characteristics of rapid response ability and robustness to uncertain parameters, among others, can be obtained using SMC.

Recently, much work regarding the use of SMC in the application of attitude control of a satellite has been reported. Kurode *et al.* [7] performed a large-angle attitude maneuver, for the first time, and performed subsequent related work in [8] and [9]. In [10], a favorable SMC algorithm was used to develop a rigid spacecraft. In the theoretical analysis, the proposed attitude tracking controller considered the issue of external disturbances. In [11], a sliding mode feedback controller was presented to investigate a rotational maneuver for a flexible satellite. Moreover, an adaptive tracking control issue is also concerned in this field. In the recent references [12], [13], the authors not only focus on the nonlinear Hamiltonian multi-input multi-output systems but also focus on a class of uncertain nonlinear systems, the uncertainty of the system are all dealt with adaptive tracking control. The controller was developed based on SMC, and it was verified by applying it to attitude control of

a spacecraft. Reference [13] devoted their works to study a tracking controller based an adaptive SMC technology for a flexible satellite, and the issues of inertia matrix uncertainty and external disturbance variability were all considered during the design. In [14], a disturbance observer was proposed, and an SMC was then designed to improve attitude control performance. A tracking problem was discussed based on higher order SMC in [15]. Considering actuator saturation, attitude stabilization for a spacecraft was investigated in [16]. Zhiwei Gao et al. presented an unknown input observer-based robust fault estimation concept in [17]. This observer could allow an augmented system to eliminate the partial disturbances that could not be decoupled in its own system. Zhiwei Gao et al. presented another fault estimation concept in [4]; a fault tolerance controller was designed by using the correct estimation error dynamics. In [4], two SMC observers were presented to realize the uncertainty fault estimation, and the traditional sliding surface switching issue was avoided at the same time.

Most of the former works either focus on the uncertainties in the satellite inertia or focus on the assumption that a precise actuator model exists. This assumption is not perfect because of the uncertainties of the actuator parameters that derive from installation error, aging components, etc. The actuator faults represent the first type uncertainty for an actuator that should be addressed [18]. In addition, the possibility of malfunctions in actuators will be increased because of the challenging operating conditions [19]. This issue will lead to some problems, such as economic, environmental and safety problems. In recent literature reports, an SMC with actuator faults is not yet the research focus. However, not only the reliable attitude stabilization was achieved by an SMC based controller but also an adaptive SMC control approach was proposed. In addition, good attitude tracking maneuvers could be performed [14]. Considering the disturbances and thruster failures of spacecraft, [20] presented another adaptive SMC attitude controller. Considering the unknown faults caused by rotating solar flap faults and weight loss of satellite mass distribution, [21] presented a terminal SMCC(TSMCC) for satellite formations flying. Reference [22] developed an SMCC to accomplish attitude tracking for a flexible satellite, although partial failure of the actuators occurred. In [20], an adaptive SMC attitude controller was proposed under multi-uncertainty of the actuator.

Actuator misalignment is another type of actuator uncertainty issue that was solved in [21]. Some actuators alignment error still exists for some special problems during launch, and this alignment error may cause the control algorithm to fail. To handle actuator misalignments, a good control methodology is required. Unfortunately, the research regarding the control of actuator misalignments is scarce. Reference [25] devoted their work to accomplish attitude maneuver based on an adaptive control law; this idea originated from the relative small gimbals' installation deviation of variable speed control moment gyros. Reference [22] proposed an adaptive control scheme based nonlinear model reference with fifteen degrees alignment errors. Reference [27] presented an extended Kalman filter without uncertain inertia properties for an on-orbit actuator alignment calibration. Focusing on the issue, magnitude error and misalignment of thrust, for satellite formation flying, a special adaptive controller was presented. In addition, some researchers addressed a series of intelligent FD approaches, dislocated time series convolutional neural architecture [23], and a just-in-time learning-based data driven approach [24].

Although the preceding SMC attitude control approaches can accomplish attitude maneuvers, the system states can only asymptotically reach the equilibrium point at infinite time. That infinite settling time, however, is not an ideal option during critical phases of missions that have some high real-time requirements [25]. It is well known that a military satellite has the stringent requirements to provide coverage of a specific high priority area. Ground objectives may be lost if the attitude of the satellite cannot be stabilized in a finite period. Therefore, a finite-time control strategy has been devised and applied to the satellite attitude system [26]. Recently, SMC has been developed as an effective method for finite-time stabilization. In [27], the attitude tracking problem was investigated by using terminal SMC (TSMC). The proposed controller guaranteed that a given desired attitude motion can be achieved in a finite time period, despite model uncertainties and disturbances. In [28], a discontinuous finite-time control law was devised for a rigid satellite to govern the attitude to be within a small region of the origin. The approach was based on TSMC, and external disturbances were considered. In [29], a robust TSMC design was presented to achieve attitude tracking deviation convergence in finite-time. In [14], a TSMC scheme was proposed to guarantee the stabilization of attitude in a finite period. More recently, a global saturated finite-time control strategy was developed in [30]. The controller was synthesized based on a homogeneous method that addresses actuator saturation.

The acceleration direction can be effectively controlled if the satellite is equipped with thrusters [31], implying that the maneuverability of the satellite can be significantly improved for a satellite operating in space. Motivated by TSMC, a TSMC control strategy was presented. In the control design, external disturbances and thruster faults were exactly reconstructed by an equivalent output injection sliding mode observer [14]. Next, a terminal SMCC (TSMCC) was synthesized via the estimated information and the system states. The main contribution of this study is that, compared with the aforementioned studies associated with SMC or proportional integral derivative (PID) controls, the proposed approach could stabilize the attitude in a finite period, while actuator uncertainties including actuator faults and actuator misalignment are addressed simultaneously. Because the attitude cannot be stabilized by conventional PID and SMC control schemes within a limited time, the finite-time attitude stabilization obtained from the proposed approach means that the designed controller is able to provide a faster response than conventional PID and SMC control. Consequently, the

developed control can provide more coverage of a specific high priority area and take many more images than conventional PID and SMC.

This paper is composed of five parts. The rigid satellite mathematical model equipped with thrusters and the problem formulations are presented in section 2. In section 3, an SMCC approach is proposed to perform attitude stabilization with finite-time convergence. Some examples for the satellite to confirm the proposed control are described in section 4. The conclusions of this paper are presented in section 5.

## II. SYSTEM DESCRIPTION AND PROBLEM FORMULATION

Let $||\cdot||$ denote the standard Euclidean norm of a vector induced norm of a matrix. $\boldsymbol{I}_n \in \Re^{n\times n}$ is the $n$-by-$n$ identity matrix. For $\boldsymbol{x} = [\,x_1\ x_2\ \ldots\ x_n\,]^{\mathrm{T}} \in \Re^n$, a vector $\boldsymbol{sgn}(\boldsymbol{x}) = [\,sign(x_1)\ sign(x_2)\ \ldots\ sign(x_n)\,]^{\mathrm{T}}$ is defined, where $sign(\cdot)$ denotes the standard sign function.

### A. MATHEMATICAL MODEL OF A RIGID SATELLITE

Assuming the satellite is a rigid body, the satellite attitude, which is represented by Modified Rodrigues Parameters (MPRs), mathematical model can be defined via [32]

$$\dot{\boldsymbol{\sigma}} = \frac{1}{4}[(1-\boldsymbol{\sigma}^{\mathrm{T}}\boldsymbol{\sigma})\boldsymbol{I}_3 + 2\boldsymbol{\sigma}^{\times} + 2\boldsymbol{\sigma}\boldsymbol{\sigma}^{\mathrm{T}}]\boldsymbol{\omega} = \boldsymbol{G}(\boldsymbol{\sigma})\boldsymbol{\omega} \quad (1)$$

$$\boldsymbol{J}\dot{\boldsymbol{\omega}} = -\boldsymbol{\omega}^{\times}\boldsymbol{J}\boldsymbol{\omega} + \boldsymbol{u} + \boldsymbol{d} \quad (2)$$

where $\boldsymbol{J} \in \Re^{3\times3}$, $\boldsymbol{u} \in \Re^3$, and $\boldsymbol{d} \in \Re^3$ expresses the positive-definite inertia matrix, total control torque, and unknown bounded external disturbance, respectively. For any vector $\boldsymbol{\psi} = [\,\psi_1\ \psi_2\ \psi_3\,]^{\mathrm{T}}$, $\boldsymbol{\xi}^{\times}$ is a skew-symmetric matrix:

$$\boldsymbol{\psi}^{\times} = \begin{bmatrix} 0 & -\psi_3 & \psi_2 \\ \psi_3 & 0 & -\psi_1 \\ -\psi_2 & \psi_1 & 0 \end{bmatrix} \quad (3)$$

*Remark 1:* This case can be found in [33]. Here, we employed the MPRs vector $\boldsymbol{\sigma}$ and its shadow counterpart $\sigma^s$, which is defined by $\boldsymbol{\sigma}^s = -\boldsymbol{\sigma}/(\boldsymbol{\sigma}^{\mathrm{T}}\boldsymbol{\sigma})$, to express the attitude rotation.

*Assumption 1:* The disturbance $\boldsymbol{d}$ is limited and satisfied with $||\boldsymbol{d}|| \le d_{\max}(d_{\max} > 0)$.

All the primary external disturbance $\boldsymbol{d}$ are bounded for any on-orbit satellite in practice [34], i.e., Assumption 1 is reasonable. In practice, as given in [34], the upper bound $d_{\max}$ can be conservatively calculated.

### B. THRUSTER FAULTS

Assume that the satellite has $N$ thrusters, and the force component can be deduced as follows:

$$\boldsymbol{F}_i = F_i \begin{bmatrix} \cos\alpha_i \cos\beta_i \\ \cos\alpha_i \sin\beta_i \\ \sin\alpha_i \end{bmatrix} \quad (4)$$

where $i = 1, 2, \ldots, N$ and $F_i > 0$, $\alpha_i$, and $\beta_i$ denote the constant thrust level, the elevation angle, and the azimuth angle, respectively. Let $\boldsymbol{r}_i = r_{xi}\boldsymbol{X}_B + r_{yi}\boldsymbol{Y}_B + r_{zi}\boldsymbol{Z}_B$ be the vector corresponding to the location of the satellite mass center of the thruster. The calculated formula of the torque component derived from the $i^{\mathrm{th}}$ thruster is

$$\boldsymbol{\tau}_i = \boldsymbol{r}_i \times \boldsymbol{F}_i \quad (5)$$

Moreover, the application of control torque $\boldsymbol{u}$ provided by $N$ thrusters can be calculated as

$$\boldsymbol{u} = \sum_{i=1}^{N} \boldsymbol{\tau}_i = \sum_{i=1}^{N} \boldsymbol{r}_i \times \boldsymbol{F}_i \quad (6)$$

In this paper, thruster faults not only include misalignment error but also include thrust magnitude error. The following are descriptions of the nature of the two scenarios:

#### 1) MISALIGNMENT ERROR

For a thruster, misalignment error may exist in $\boldsymbol{r}_i$ and the alignment angles $\alpha_i$ and $\beta_i$. Let $\boldsymbol{r}_i^n$ and $\Delta\boldsymbol{r}_i$ represent the nominal value and the misalignment error between satellite center and the thruster, respectively. Thus, $\boldsymbol{r}_i$ can be expressed as $\boldsymbol{r}_i = \boldsymbol{r}_i^n + \Delta\boldsymbol{r}_i$. We assume that the thruster is used over a nominal direction with small constant angles, $\Delta\alpha_i$ and $\Delta\beta_i$. Consequently, the alignment angle can be represented using the formulas $\alpha_i = \alpha_i^n + \Delta\alpha_i$ and $\beta_i = \beta_i^n + \Delta\beta_i$, where $\alpha_i^n$ and $\beta_i^n$ denote the nominal alignment angle.

#### 2) THRUST MAGNITUDE ERROR

As reported in [35], the amount of thrust generated will be reduced according to the propellant's mass lost. Let $F_n$ and $\Delta F_i$ denote the nominal value and thrust magnitude error, respectively. Thus, the actual thrust $F_i$ can be represented by

$$F_i = F_n + \Delta F_i \quad (7)$$

For the physical limitation of the thruster, the actual thrust $F_i$ generated is positive, and its maximum thrust should meet the conditions $0 \le F_i \le F_n$. Hence, the error of the thrust magnitude $\Delta F_i$ is such that $-F_n \le \Delta F_i \le 0$. The case when $\Delta F_i = 0$ indicates that the $i^{\mathrm{th}}$ thruster operates normally. The case of $\Delta F_i = -F_n$ denotes that the $i^{\mathrm{th}}$ thruster is completely lost and is valid. The case of $-F_n < \Delta F_i < 0$ corresponds to the status in which the thrust of the $i^{\mathrm{th}}$ thruster partially loses its effectiveness.

Considering the thruster faults, $\tau_i$ in (5) can be rewritten as

$$\begin{aligned}\boldsymbol{\tau}_i &= (F_n + \Delta F_i)(\boldsymbol{r}_i^n + \Delta\boldsymbol{r}_i) \\ &\quad \times \begin{bmatrix} \cos(\alpha_i^n + \Delta\alpha_i)\cos(\beta_i^n + \Delta\beta_i) \\ \cos(\alpha_i^n + \Delta\alpha_i)\sin(\beta_i^n + \Delta\beta_i) \\ \sin(\alpha_i^n + \Delta\alpha_i) \end{bmatrix} \\ &= F_n(\boldsymbol{r}_i^n)\times\boldsymbol{D}_i^n + \Delta F(\boldsymbol{r}_i^n) \times \boldsymbol{D}_i^n + (F_n + \Delta F_i)[(\boldsymbol{r}_i^n) \times \Delta\boldsymbol{D}_i^n \\ &\quad + \Delta\boldsymbol{r}_i \times (\boldsymbol{D}_i^n + \Delta\boldsymbol{D}_i^n)] \end{aligned} \quad (8)$$

$$\boldsymbol{u} = \underbrace{F_n \sum_{i=1}^{N} (r_i^n) \times \boldsymbol{D}_i^n}_{u_n} + \underbrace{\sum_{i=1}^{N} \{\Delta F(r_i^n) \times \boldsymbol{D}_i^n + (F_n + \Delta F_i)[(r_i^n) \times \Delta \boldsymbol{D}_i^n + \Delta r_i \times (\boldsymbol{D}_i^n + \Delta \boldsymbol{D}_i^n)]\}}_{u_f} \tag{11}$$

where

$$\boldsymbol{D}_i^n = \begin{bmatrix} \cos\alpha_i^n \cos\beta_i^n \\ \cos\alpha_i^n \sin\beta_i^n \\ \sin\alpha_i^n \end{bmatrix} \tag{9}$$

$$\Delta \boldsymbol{D}_i^n = \begin{bmatrix} \cos(\alpha_i^n + \Delta\alpha_i)\cos(\beta_i^n + \Delta\beta_i) \\ \cos(\alpha_i^n + \Delta\alpha_i)\sin(\beta_i^n + \Delta\beta_i) \\ \sin(\alpha_i^n + \Delta\alpha_i) \end{bmatrix} - \begin{bmatrix} \cos\alpha_i^n \cos\beta_i^n \\ \cos\alpha_i^n \sin\beta_i^n \\ \sin\alpha_i^n \end{bmatrix} \tag{10}$$

From (6) and (8), considering both the magnitude error and misalignment, the total thrust force can be defined by (11), as shown at the top of this page, which expresses the sum of the nominal values and the thrust error terms.

Where $\boldsymbol{u}_n \in \Re^3$ represents the nominal control torque caused by the controller, and $\boldsymbol{u}_f \in \Re^3$ represents the faulty torque caused by the two main errors indicated above.

*Assumption 2:* The faulty torque $\boldsymbol{u}_f$ introduced by thruster faults is bounded by a positive scalar $u_{\max}$, *i.e.*, $||\boldsymbol{u}_f|| \leq u_{\max}$.

*Remark 2:* Because of the physical limitation of the thruster, it should have $|\Delta F_i| \leq F_n$. Although the manufacturing technique is finite, the inequality $||\Delta \boldsymbol{r}_i|| \leq ||\boldsymbol{r}_i^n||$ can always be guaranteed. Hence, it follows that

$$\begin{aligned} ||u_f|| &\leq \sum_{i=1}^{N} ||\Delta F(r_i^n) \times \boldsymbol{D}_i^n + (F_n + \Delta F_i) \\ &\quad \times [(r_i^n) \times \Delta \boldsymbol{D}_i^n + \Delta \boldsymbol{r}_i \times (\boldsymbol{D}_i^n + \Delta \boldsymbol{D}_i^n)]|| \\ &\leq F_n \sum_{i=1}^{N} [||(r_i^n) \times \boldsymbol{D}_i^n|| + 2||(r_i^n) \times \Delta \boldsymbol{D}_i^n \\ &\quad + \Delta \boldsymbol{r}_i \times (D_i^n + \Delta \boldsymbol{D}_i^n)||] \end{aligned} \tag{12}$$

Moreover, it can be obtained from (10) that $||\Delta {D_i}^n|| \leq 2\sqrt{3}$. Hence, (12) becomes

$$||\boldsymbol{u}_f|| \leq F_n \sum_{i=1}^{N} \{||(r_i^n) \times \boldsymbol{D}_i^n|| + 2[2\sqrt{3}||\boldsymbol{r}_i^n|| + ||\boldsymbol{r}_i^n||||\boldsymbol{D}_i^n + 2\sqrt{3}||]\} \tag{13}$$

From (13), Assumption 2 is therefore reasonable because $\boldsymbol{u}_f$ is bounded by (13) at most.

### C. PROBLEM FORMULATION

The following states are the control objective to be achieved: Consider the rigid satellite attitude system represented by (1)-(2) with external disturbances and thruster faults, design a control input $\boldsymbol{u}_n$ to stabilize the attitude in finite-time. In other words, the attitude $\boldsymbol{\sigma}$ and the angular velocity $\dot{\boldsymbol{\sigma}}$ are governed to zero in finite-time.

## III. MAIN RESULT

A sliding mode attitude controller will be presented for attitude stabilization. For the first step of the control design, a sliding mode observer is employed to estimate the external disturbances and thruster faults. The design of the observer is derived from an equivalent control approach. The estimation is accomplished in finite-time with zero estimation error. Next, a sliding mode attitude controller will be synthesized by utilizing the reconstructed information and system states.

### A. ESTIMATION OF FAULTS WITH SLIDING MODE OBSERVER

Define a matrix $\boldsymbol{T}(\boldsymbol{\sigma}) = \boldsymbol{G}^{-1}(\boldsymbol{\sigma})$; the following dynamics can be obtained from (1)-(2) with thruster faults (11):

$$\bar{\boldsymbol{J}}(\boldsymbol{\sigma})\ddot{\boldsymbol{\sigma}} + \boldsymbol{C}(\boldsymbol{\sigma}, \dot{\boldsymbol{\sigma}})\dot{\boldsymbol{\sigma}} = \boldsymbol{T}^{\mathrm{T}}\boldsymbol{u}_n + \boldsymbol{T}^{\mathrm{T}}(\boldsymbol{u}_f + \boldsymbol{d}) \tag{14}$$

where $\bar{\boldsymbol{J}}(\boldsymbol{\sigma}) = T^{\mathrm{T}}JT$, and $\boldsymbol{C}(\boldsymbol{\sigma}, \dot{\boldsymbol{\sigma}}) = \boldsymbol{T}^{\mathrm{T}}\boldsymbol{J}\dot{\boldsymbol{T}} + \boldsymbol{T}^{\mathrm{T}}(\boldsymbol{T}\dot{\boldsymbol{\sigma}})^{\times}\boldsymbol{J}\boldsymbol{T}$. The dynamic model (14) is represented by the three properties mentioned below:

**P1.** The matrix $\boldsymbol{G}(\boldsymbol{\sigma})$ is defined to be the same as [32]:

$$\begin{aligned} \boldsymbol{T}(\boldsymbol{\sigma}) &= \frac{16}{(1 + \boldsymbol{\sigma}^{\mathrm{T}}\boldsymbol{\sigma})^2}\boldsymbol{G}^{\mathrm{T}}(\boldsymbol{\sigma}), \\ \boldsymbol{G}^{\mathrm{T}}(\boldsymbol{\sigma})\boldsymbol{G}(\boldsymbol{\sigma}) &= (\frac{1 + \boldsymbol{\sigma}^{\mathrm{T}}\boldsymbol{\sigma}}{4})^2\boldsymbol{I}_3 \end{aligned} \tag{15}$$

**P2**: The matrix $\bar{\boldsymbol{J}}(\boldsymbol{\sigma})$ is positive-definite and symmetric.

**P3**: The matrix $\boldsymbol{C}(\boldsymbol{\sigma}, \dot{\boldsymbol{\sigma}})$ and the time-derivative of $\bar{\boldsymbol{J}}(\boldsymbol{\sigma})$ satisfy the skew-symmetric relationship [10]: $\boldsymbol{x}^{\mathrm{T}}(\dot{\bar{\boldsymbol{J}}}(\boldsymbol{\sigma}) - 2\boldsymbol{C}(\boldsymbol{\sigma}, \dot{\boldsymbol{\sigma}}))\boldsymbol{x} = 0$ for all $\boldsymbol{x} \in \Re^3$.

To reconstruct external disturbances and thruster faults, a new variable is defined as $\bar{\boldsymbol{u}} = \boldsymbol{T}^{\mathrm{T}}(\boldsymbol{u}_f + \boldsymbol{d})$. Thus, if $\bar{\boldsymbol{u}}$ can be precisely reconstructed, then $\boldsymbol{u}_f + \boldsymbol{d}$ can be exactly reconstructed. The problem is thus changed into the estimation of $\bar{\boldsymbol{u}}$. To reconstruct $\bar{\boldsymbol{u}}$ using only system states (*i.e.*, $\boldsymbol{\sigma}$ and $\dot{\boldsymbol{\sigma}}$) and the available nominal control $\boldsymbol{u}_n$, a residual vector is defined as

$$\boldsymbol{r}(t) = -\eta \boldsymbol{J}_t + \eta \int_0^t [\boldsymbol{T}^{\mathrm{T}}\boldsymbol{u}_n + \boldsymbol{H}_2(\boldsymbol{\sigma}, \dot{\boldsymbol{\sigma}}) - \boldsymbol{r}(\varsigma)]d\varsigma \tag{16}$$

where $\eta$ is a positive scalar, $\boldsymbol{J}_t = \bar{\boldsymbol{J}}(\boldsymbol{\sigma})\dot{\boldsymbol{\sigma}}$, and $\boldsymbol{H}_2(\boldsymbol{\sigma}, \dot{\boldsymbol{\sigma}}) = \dot{\bar{\boldsymbol{J}}}(\boldsymbol{\sigma})\dot{\boldsymbol{\sigma}} - C(\boldsymbol{\sigma}, \dot{\boldsymbol{\sigma}})\dot{\boldsymbol{\sigma}}$. Because $\boldsymbol{J}_t$, $\boldsymbol{u}_n$, and $\boldsymbol{H}_2(\boldsymbol{\sigma}, \dot{\boldsymbol{\sigma}})$ are computable, $\boldsymbol{r}(t)$ can be exactly obtained. Using (14) and P2-P3, the signal $\boldsymbol{r}(t)$ is such that

$$\dot{\boldsymbol{r}} = -\eta \boldsymbol{r} - \eta \bar{\boldsymbol{u}} \tag{17}$$

For the linear system (17), a sliding mode observer is proposed using the measurable state $\boldsymbol{r}$:

$$\dot{\hat{\boldsymbol{x}}}_1 = -\eta\hat{\boldsymbol{x}}_1 - \lambda_1\boldsymbol{e} - \lambda_2\boldsymbol{sgn}(\boldsymbol{e}) \tag{18}$$

where $\hat{\boldsymbol{x}}_1$ is the estimate of $\boldsymbol{r}$, $\boldsymbol{e} = \hat{\boldsymbol{x}}_1 - \boldsymbol{r}$ is the estimated error, and $\lambda_i$, $i = 1, 2$ are positive scalars.

*Theorem 1:* Consider the linear system (17) with the sliding mode observer (18). If $\lambda_2$ is chosen such that

$$\lambda_2 - 4\eta(u_{\max} + d_{\max}) > 0 \tag{19}$$

then $\bar{\boldsymbol{u}}(t)$ can be reconstructed exactly in finite-time $T_r = ||\boldsymbol{e}(0)||/\pi$. Moreover, the amplitude of external disturbances and thruster faults (*i.e.*, $\boldsymbol{u}_f + \boldsymbol{d}$) can be reconstructed after finite-time $T_r$ with zero estimation error.

*Proof:* The dynamic equation for the error $\boldsymbol{e}$ can be obtained from (17) and (18), that is,

$$\dot{\boldsymbol{e}} = -(\eta + \lambda_1)\boldsymbol{e} - \lambda_2\boldsymbol{sgn}(\boldsymbol{e}) + \eta\bar{\boldsymbol{u}} \tag{20}$$

Consider a Lyapunov candidate function as

$$V_1(t) = 0.5\boldsymbol{e}^{\mathrm{T}}\boldsymbol{e} \tag{21}$$

Hence,

$$\begin{aligned}\dot{V}_1 &= \boldsymbol{e}^{\mathrm{T}}[-(\eta + \lambda_1)\boldsymbol{e} - \lambda_2\boldsymbol{sgn}(\boldsymbol{e}) + \eta\bar{\boldsymbol{u}}] \\ &\le -(\eta + \lambda_1)||\boldsymbol{e}||^2 - (\lambda_2 - \eta||\bar{\boldsymbol{u}}||)||\boldsymbol{e}||\end{aligned} \tag{22}$$

Using Remark 1 and (15) in P1, it follows that

$$||\boldsymbol{T}(\boldsymbol{\sigma})|| = \frac{16}{(1 + \boldsymbol{\sigma}^{\mathrm{T}}\boldsymbol{\sigma})^2}||G^{\mathrm{T}}(\boldsymbol{\sigma})|| \le 4 \tag{23}$$

Applying (23) and Assumptions 1-2 yields the following:

$$||\bar{\boldsymbol{u}}|| \le ||\boldsymbol{T}^{\mathrm{T}}||||(\boldsymbol{u}_f + \boldsymbol{d})|| \le 4(u_{\max} + d_{\max}) \tag{24}$$

Let $\lambda_2 - 4\eta(u_{\max} + d_{\max})$ be equal to $\pi$, *i.e.*, $\lambda_2 - 4\eta(u_{\max} + d_{\max}) = \pi$; with the choice of $\lambda_2$ in (19), (22) becomes

$$\dot{V}_1 \le -\pi||\boldsymbol{e}|| \tag{25}$$

Defining a continuous function $W_1(t) = \sqrt{2V_1(t)} = ||\boldsymbol{e}||$, one has

$$\dot{W}_1(t) = \frac{\dot{V}_1(t)}{\sqrt{2V_1(t)}} \le -\pi\frac{||\boldsymbol{e}||}{\sqrt{2V_1(t)}} = -\pi \tag{26}$$

Based the comparison theorem mentioned in [36], it is certain from (26) that

$$W_1(t) \le W_1(e_1(0)) - \pi t \tag{27}$$

The definition of $W_1(t)$ and (27) lead to $||\boldsymbol{e}(t)|| \equiv 0$ for all $t \ge T_r$. Therefore, the sliding motion occurs on $\boldsymbol{e} = \dot{\boldsymbol{e}} = \boldsymbol{0}$ by the time $t = T_r$. If the state reaches the sliding surface $\boldsymbol{e} = \dot{\boldsymbol{e}} = \boldsymbol{0}$, the equivalent output injection yields will be handled

$$\bar{\boldsymbol{u}}(t) = \frac{1}{\eta}(\lambda_2\boldsymbol{sgn}(\boldsymbol{e}))_{eq}, \quad t \ge T_r \tag{28}$$

Hence, $\bar{\boldsymbol{u}}(t)$ is exactly reconstructed by $(\lambda_2\boldsymbol{sgn}(\boldsymbol{e}))_{eq}/\eta$ after finite-time $T_r$. Consequently, $\boldsymbol{u}_f + \boldsymbol{d}$ can be reconstructed by using (29) in finite-time $T_r$ with zero estimation error:

$$\boldsymbol{u}_f + \boldsymbol{d} \equiv \boldsymbol{G}^{\mathrm{T}}(\boldsymbol{\sigma})\bar{\boldsymbol{u}} \equiv \frac{1}{\eta}\boldsymbol{G}^{\mathrm{T}}(\boldsymbol{\sigma})(\lambda_2\boldsymbol{sgn}(\boldsymbol{e}))_{eq}, \quad t \ge T_r \tag{29}$$

According to a low pass filtering operation of $\lambda_2\boldsymbol{sgn}(\boldsymbol{e})$, the equivalent control can be obtained [37]. ■

### B. DESIGN FOR A SLIDING MODE ATTITUDE CONTROLLER WITH FINITE-TIME CONVERGENCE

Here, an SMCC is proposed for attitude stabilization. A sliding surface with a reaching law should be selected as the first step in the control design. A fast terminal sliding surface will be defined as follows according to the information regarding attitude and angular velocity:

$$\boldsymbol{S} = [\,S_1\ S_2\ S_3\,]^{\mathrm{T}} = \dot{\boldsymbol{\sigma}} + \alpha_1\boldsymbol{\sigma} + \beta_1|\boldsymbol{\sigma}|^{\gamma_1}\boldsymbol{sgn}(\boldsymbol{\sigma}) \tag{30}$$

where $\alpha_1$, $\beta_1$, and $0 < \gamma_1 < 1$ are positive scalars, $|\boldsymbol{\sigma}|^{\gamma_1} = diag([\,|\sigma_1|^{\gamma_1}\ |\sigma_2|^{\gamma_1}\ |\sigma_3|^{\gamma_1}\,])$.

For the SMC design, the control input usually has a structure of

$$\boldsymbol{u}_n = \boldsymbol{u}_{eq} + \boldsymbol{u}_{disc} \tag{31}$$

where $\boldsymbol{u}_{eq}$ is an equivalent control to confirm sliding surface $S$ constant, and it can be handled by setting $\dot{\boldsymbol{S}}, \boldsymbol{S}$ to zero. $\boldsymbol{u}_{disc}$ is a discontinuous control effort that governs the states to reach the sliding surface.

To achieve finite-time reaching the sliding surface, here, we employ a control law defined by [38]:

$$\dot{\boldsymbol{S}} = -\frac{K}{\chi(\boldsymbol{S})}\boldsymbol{sgn}(\boldsymbol{S}) \tag{32}$$

where

$$\begin{aligned}\frac{K}{\chi(\boldsymbol{S})} = diag([&\frac{K}{\varepsilon_0 + (1-\varepsilon_0)e^{-\alpha_2||S_1||^{\gamma_2}}} \\ &\frac{K}{\varepsilon_0+(1-\varepsilon_0)e^{-\alpha_2||S_2||^{\gamma_2}}}\ \frac{K}{\varepsilon_0+(1-\varepsilon_0)e^{-\alpha_2||S_3||^{\gamma_2}}}]),\\ &K > 0\end{aligned}$$

is a scalar, $\varepsilon_0$ represents a strictly positive offset that is less than one, $\alpha_2$ and $\gamma_2$ are strictly positive integers.

*Theorem 2:* For the satellite attitude system (1)-(2) with thruster faults and disturbances, design $\boldsymbol{u}_{eq}$ and $\boldsymbol{u}_{disc}$ as follows:

$$\begin{aligned}\boldsymbol{u}_{eq} = \boldsymbol{G}^{\mathrm{T}}(\boldsymbol{\sigma})[&-\boldsymbol{C}(\boldsymbol{\sigma}, \dot{\boldsymbol{\sigma}})\dot{\boldsymbol{\sigma}} - \frac{1}{\eta}(\lambda_2\boldsymbol{sgn}(\boldsymbol{e}))_{eq} \\ &-\bar{\boldsymbol{J}}(\boldsymbol{\sigma})(\alpha_1\boldsymbol{I}_3 + \beta_1\gamma_1|\boldsymbol{\sigma}|^{\gamma_1-1})\boldsymbol{G}(\boldsymbol{\sigma})\boldsymbol{\omega}]\end{aligned} \tag{33}$$

$$\boldsymbol{u}_{disc} = -\boldsymbol{G}^{\mathrm{T}}(\boldsymbol{\sigma})\bar{\boldsymbol{J}}(\boldsymbol{\sigma})\frac{K}{\chi(\boldsymbol{S})}\boldsymbol{sgn}(\boldsymbol{S}) \tag{34}$$

With the application of the control structure (31), the states of the system can reach the sliding surface $\boldsymbol{S} = 0$ in a finite period. Moreover, the controller will govern the angular velocity and the attitude reaching the equilibrium point $\boldsymbol{\sigma} = \boldsymbol{0}$ and $\boldsymbol{\omega} = \boldsymbol{0}$ in a finite period, separately.

*Proof:* For representing the stability with finite-time convergence, we first prove finite-time convergence of $S$ and then show a corresponding proof for $\boldsymbol{\sigma}$ and $\boldsymbol{\omega}$.

#### 1) FINITE-TIME CONVERGENCE OF $S$

Here, a candidate Lyapunov function $V_2 = 0.5\boldsymbol{S}^{\mathrm{T}}\boldsymbol{S}$ is employed. Applying (1) and (14), the time-derivative of $V_2$ is defined by

$$\begin{aligned}\dot{V}_2 &= \boldsymbol{S}^{\mathrm{T}}(\ddot{\boldsymbol{\sigma}} + \alpha_1\dot{\boldsymbol{\sigma}} + \beta_1\gamma_1|\boldsymbol{\sigma}|^{\gamma_1-1}\dot{\boldsymbol{\sigma}}) \\ &= \boldsymbol{S}^{\mathrm{T}}\{\bar{\boldsymbol{J}}^{-1}(\boldsymbol{\sigma})[-C(\boldsymbol{\sigma},\dot{\boldsymbol{\sigma}})\dot{\boldsymbol{\sigma}} + T^{\mathrm{T}}\boldsymbol{u}_n \\ &= +\boldsymbol{T}^{\mathrm{T}}(\boldsymbol{u}_f + \boldsymbol{d})] + (\alpha_1\boldsymbol{I}_3 + \beta_1\gamma_1|\boldsymbol{\sigma}|^{\gamma_1-1})\boldsymbol{G}(\boldsymbol{\sigma})\boldsymbol{\omega}\} \quad (35)\end{aligned}$$

Inserting (33)-(34) yields

$$\begin{aligned}\dot{V}_2 = \boldsymbol{S}^{\mathrm{T}}[-\frac{K}{\chi(\boldsymbol{S})}\boldsymbol{sgn}(\boldsymbol{S}) - \frac{1}{\eta}\bar{\boldsymbol{J}}^{-1}(\boldsymbol{\sigma})(\lambda_2\boldsymbol{sgn}(\boldsymbol{e}))_{eq} \\ + \bar{\boldsymbol{J}}^{-1}(\boldsymbol{\sigma})\boldsymbol{T}^{\mathrm{T}}(\boldsymbol{u}_f + \boldsymbol{d})] \quad (36)\end{aligned}$$

As proved in Theorem 1, $\bar{\boldsymbol{u}} = \boldsymbol{T}^{\mathrm{T}}(\boldsymbol{u}_f + \boldsymbol{d}) \equiv \frac{1}{\eta}(\lambda_2\boldsymbol{sgn}(\boldsymbol{e}))_{eq}$ holds for all $t \geq T_r$. Hence, it follows from the definition of $K/\chi(\boldsymbol{S})$ in (32) that

$$\begin{aligned}\dot{V}_2 &= -\boldsymbol{S}^{\mathrm{T}}\frac{K}{\chi(\boldsymbol{S})}\boldsymbol{sgn}(\boldsymbol{S}) = -K\sum_{i=1}^{3}\frac{|S_i|}{\varepsilon_0 + (1-\varepsilon_0)e^{-\alpha_2||S_i||^{\gamma_2}}} \\ &\leq -\frac{K}{\varepsilon_0}\sum_{i=1}^{3}|S_i| = -\frac{\sqrt{2}K}{\varepsilon_0}\sqrt{V_2} \quad (37)\end{aligned}$$

Hence, it can be established from (37) that $\lim_{t\to\infty} V_2(t) = 0$. With the definition of $V_2(t)$, $\lim_{t\to\infty} S(t) = 0$ is guaranteed.

Furthermore, it can be obtained from the exponential reaching law (32) that

$$\dot{S}_i = -\frac{K}{\varepsilon_0 + (1-\varepsilon_0)e^{-\alpha_2||S_i||^{\gamma_2}}}sign(S_i) \quad (38)$$

As proved in [38], solving (37) yields that $|S_i(t)| \equiv 0$ for all $t \geq T_{si}$, where $T_{si}$ is given by

$$T_{si} = \frac{1}{K}[\varepsilon_0|S_i(0)| + (1-\varepsilon_0)\int_0^{|S_i(0)|} e^{-\alpha_2|S_i|^{\gamma_2}}dS_i] \quad (39)$$

In a finite-time $T_s = \max_{i=1,2,3} T_{si}$; thus, all the states of the attitude system can reach the sliding surface $\boldsymbol{S}$, that is, $\boldsymbol{S}(t) \equiv 0$ for all $t \geq T_s$.

#### 2) FINITE-TIME CONVERGENCE OF $\sigma$ AND $\omega$

When all the states are driven onto $\boldsymbol{S} = \boldsymbol{0}$ after finite period $T_s$, (30) becomes

$$\boldsymbol{S} = \dot{\boldsymbol{\sigma}} + \alpha_1\boldsymbol{\sigma} + \beta_1|\boldsymbol{\sigma}|^{\gamma_1}\boldsymbol{sgn}(\boldsymbol{\sigma}) = \boldsymbol{0} \quad (40)$$

According to the stability criterion regarding the finite period presented in [39], it can be obtained from (40) that $\sigma_i$ will converge to zero in a finite period $T_{fi}$:

$$T_{fi} = T_{si} + \frac{1}{\alpha_1(1-\gamma_1)}\ln\frac{\alpha_1||\sigma_i(T_{si})||^{1-\gamma_1} + \beta_1}{\beta_1} \quad (41)$$

Thus, the satellite attitude $\boldsymbol{\sigma}$ converges to $\boldsymbol{\sigma} = \boldsymbol{0}$ in a finite period $T_f = \max_{i=1,2,3} T_{fi}$. In addition, applying $\boldsymbol{\sigma} = \boldsymbol{0}$ and (40) lead to $\dot{\boldsymbol{\sigma}} = \boldsymbol{0}$ for all $t \geq T_f$, and then $\boldsymbol{\omega} = \boldsymbol{0}$ is obtained.

Summarizing the above analysis, the following is established:

$$\boldsymbol{\sigma}(t) \equiv \boldsymbol{0}, \quad \boldsymbol{\omega}(t) \equiv \boldsymbol{0}, \ t \geq T_f \quad (42)$$

Therefore, the angular velocity and attitude are governed to zero in finite-time $T_f$, the attitude stabilization is accomplished in a finite period. The proof is completed. ■

## IV. SIMULATION RESULTS

To demonstrate the effectiveness of the presented controller, an example of a rigid satellite is considered, and multiple simulations are performed. The principal moments of inertia of the considered satellite are $J_{11} = 45$ kgm$^2$, $J_{22} = 50$ kgm$^2$, and $J_{33} = 47.5$ kgm$^2$. The inertia products are smaller than 0.5 kgm$^2$. To illustrate the robustness towards external disturbance torque, $\boldsymbol{d}$ is assumed as follows:

$$\boldsymbol{d} = \begin{bmatrix} 5\cos(0.2\pi t) \\ -3\cos(0.2\pi t) \\ 2\cos(0.2\pi t) \end{bmatrix} \times 10^{-3}\ \mathrm{Nm} \quad (43)$$

The satellite has twelve thrusters. Those twelve thrusters are assumed to be symmetrically distributed on three axes of $\mathcal{F}_b$. The distribution matrix can be determined simply by the distance $\boldsymbol{r}_i^{\boldsymbol{n}}$ when the propulsion force is perpendicular to the corresponding axis. Fig. 1 is the mechanical configuration of the thrusters. Pulse delay and duration are used for the thrusters, which can provide a nominal force $\boldsymbol{F_n}$ of 1 N. Table 1 lists the relative data of the nominal positions and orientation of the thrusters.

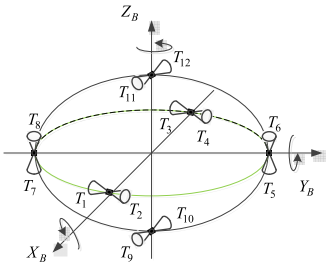


**FIGURE 1.** Distribution schematic of the six thrusters.

In our simulation, the initial conditions of the quaternion and the angular velocity are $\boldsymbol{\sigma}(0) = [0.288\ -0.143\ -0.020]^{\mathrm{T}}$ and $\boldsymbol{\omega}(0) = [-1\ 0.8\ 0.4]^{\mathrm{T}}$ rad/sec, respectively. The parameters for the controller are chosen as $\boldsymbol{\alpha_1} = 1.2$, $\boldsymbol{\alpha_2} = 0.6$, $\boldsymbol{\beta_1} = 2.5$, $\boldsymbol{\gamma_1} = 0.8$, $\boldsymbol{\gamma_2} = 0.38$, $\boldsymbol{\varepsilon_0} = 0.75$, and $\boldsymbol{K} = 0.15$. The parameters for the sliding mode observer are selected as $\boldsymbol{\eta} = 7.5$, $\boldsymbol{\lambda_1} = 0.015$, and $\boldsymbol{\lambda_2} = 0.2$.

### A. ACTUATOR UNCERTAINTIES

To investigate the controller performance, actuator uncertainties are considered. The following fault scenarios and misalignments are introduced:

**TABLE 1. Thruster's layout.**

| Thruster No | Position in $\mathcal{F}_b$ of the attitude control | | | Orientation in $\mathcal{F}_b$ | |
|---|---|---|---|---|---|
| | $r_{xi}^n$ (mm) | $r_{yi}^n$ (mm) | $r_{zi}^n$ (mm) | $\alpha_i^n$ | $\beta_i^n$ |
| $T_1$ | 700 | 0 | 0 | 0 | -90 |
| $T_2$ | 700 | 0 | 0 | 0 | 90 |
| $T_3$ | -700 | 0 | 0 | 0 | -90 |
| $T_4$ | -700 | 0 | 0 | 0 | 90 |
| $T_5$ | 0 | 800 | 0 | -90 | 90 |
| $T_6$ | 0 | 800 | 0 | 90 | 90 |
| $T_7$ | 0 | -800 | 0 | -90 | 90 |
| $T_8$ | 0 | -800 | 0 | 90 | 90 |
| $T_9$ | 0 | 0 | -700 | 0 | 0 |
| $T_{10}$ | 0 | 0 | -700 | 0 | 180 |
| $T_{11}$ | 0 | 0 | 700 | 0 | 0 |
| $T_{12}$ | 0 | 0 | 700 | 0 | 180 |

- When the thruster is switched-on, a random misalignment corresponding to the thrust misalignment is considered. In such case, this misalignment model is just Gaussian noise on both the azimuth $\boldsymbol{\Delta\alpha_i}$ and the elevation angles $\boldsymbol{\Delta\beta_i}$, with a standard deviation of 2.5% for each.
- The supplementary position of thruster $\boldsymbol{\Delta r_i}$, $\boldsymbol{i = 1, 2, \ldots, 12}$ follows a Gaussian noise model, with a standard deviation of 4% for each.
- For the first six thrusters (*i.e.*, T1 $\sim$ T6), the force delivered is modeled with a nominal value signal of $\boldsymbol{F_n = 1}$ N deteriorated by a zero-mean Gaussian noise model with a standard deviation is 0.2 N. For the $i^{\text{th}}$ thruster, $\boldsymbol{i = 7, 8, \ldots, 12}$ the decrease in the amount of thrust caused by mass reduction is simulated. This faulty thrust $\boldsymbol{\Delta F_i}$ is modeled according to the following expression:

$$\Delta F_i = \begin{cases} \mathbf{0} & \textit{if } \boldsymbol{t < 2} \\ \mathbf{-0.08 * (t - 2)} & \textit{if } \boldsymbol{2 \le t < 12} \\ \mathbf{-0.8} & \textit{if } \boldsymbol{t \ge 12} \end{cases} \tag{44}$$

### B. CONTROL PERFORMANCE

When the attitude system is accompanied by the control method, the incorporated observer results exhibit good estimation performance. The error between $\boldsymbol{u_f + d}$ and its estimation value are represented in Fig. 2. The equivalent output injection sliding mode observer achieves a finite-time estimation of thruster faults and external disturbances. That finite period of time is approximately 6.5 seconds, *i.e.*, $\boldsymbol{T_r = 6.5}$ seconds.

Because of the precisely reconstructed information of the thruster faults and external disturbances derived from the sliding mode observer (18), the proposed control input $\boldsymbol{u_n}$ can reject external disturbances and further compensate for actuator faults completely. Consequently, the TSMCC can successfully accomplish attitude stabilization maneuver in a finite period. The resulted attitude control performance is illustrated in Fig. 3. Fig. 4 illustrates the steady-state behavior; the attitude is stabilized in a finite time period of $\boldsymbol{T_f = \max_{i=1,2,3} T_{fi} = 6.85}$ seconds, while the attitude control accuracy is $\boldsymbol{|\sigma_i| \le 2.0 \times 10^{-8}}$, $\boldsymbol{i = 1, 2, 3}$. The response of angular velocity is shown in Fig. 5. As we can see in Fig. 6, the angular velocity is finally stabilized with an accuracy of $|\omega_i| \le 1.0 \times 10^{-7}$rad/sec in finite-time $T_f = 6.85$ seconds. The corresponding commanded control torque is illustrated in Fig. 7.

To further validate the function of the presented control and to provide a comparison, simulation by using the robust adaptive fault tolerant controller (RAFTC) developed in [14]

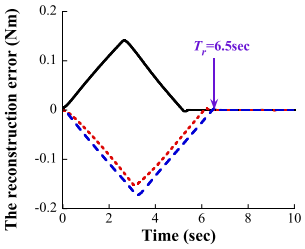


**FIGURE 2.** The estimated error between $u_f + d$ and its reconstructed value.

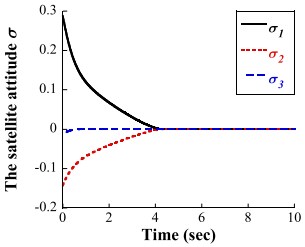


**FIGURE 3.** Time response of the attitude $\sigma$.

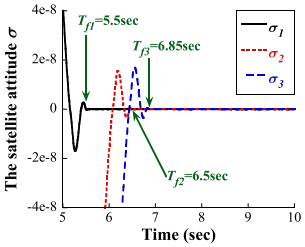


**FIGURE 4.** The steady-state behavior of the attitude $\sigma$.

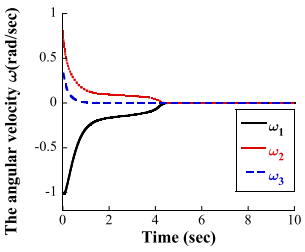


**FIGURE 5.** Time response of the angular velocity $\omega$.

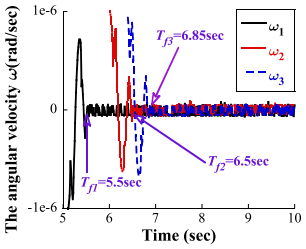


**FIGURE 6.** The steady-state behavior of the velocity $\omega$.

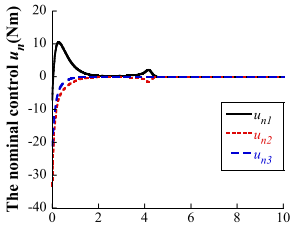


**FIGURE 7.** The nominal control $u_n$.

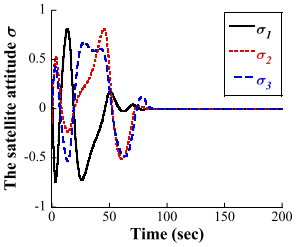


**FIGURE 8.** The attitude $\sigma$ with RAFTC.

is conducted while the satellite attitude is maneuvering. Fig. 8 represents the time response of satellite attitude with RAFTC. Its steady-state behavior is shown in Fig. 9. It is seen that the attitude of satellite can be stabilized in almost 100 seconds within $2.0 \times 10^{-4}$, *i.e.*, $|\sigma_i| \leq 2.0 \times 10^{-4}$, $i = 1, 2, 3$. The obtained angular velocity is shown in Figs. 10-11. The associated nominal control input is illustrated in Fig. 12. Moreover, the following are found:

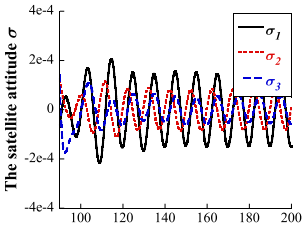


**FIGURE 9.** The steady-state behavior of the attitude $\sigma$ with RAFTC.

- Comparing Fig. 4 with Fig. 11, it is seen that time required to stabilize the attitude by the proposed control is much shorter than that of the RAFTC. Only 6.85 seconds are required for the proposed controller, whereas the RAFTC requires almost 100 seconds. This improved performance is because the proposed strategy is developed within the framework of TSMC, thus allowing it to have the capability to achieve control goal with finite-time convergence.
- From the comparison between Fig. 6 and Fig. 11, it is found that the control accuracy of angular velocity obtained from RAFTC is quite inferior to the control approach in this work because RAFTC can only guarantee that the attitude and the angular velocity converge to a small set including the origin. In contrast, the scheme presented in this article can stabilize both parameters mentioned above to zero.

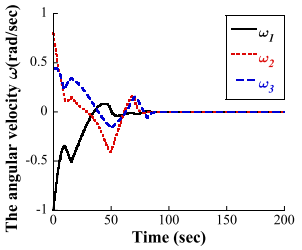


**FIGURE 10.** The angular velocity $\omega$ with RAFTC.

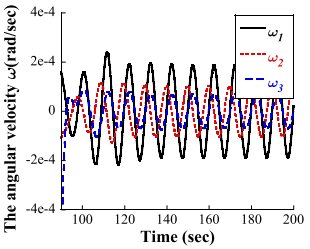


**FIGURE 11.** The steady-state behavior of $\omega$ with RAFTC.

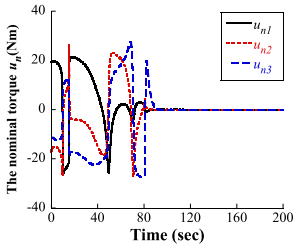


**FIGURE 12.** The nominal control $u_n$ with RAFTC.

Summarizing the above comparison results, it is obtained that the presented control scheme shows good performance compared with the controller presented in [14]. In addition, a faster response and higher pointing accuracy for the satellite can be obtained by the proposed solution.

## V. CONCLUSIONS

This paper presented a proposed sliding-mode based attitude stabilization control law for a rigid satellite. The proposed control scheme has two parts: one part involves a sliding mode observer with an equivalent output injection to reconstruct external disturbances and actuator faults, and the other part is a TSMCC. The approach has two remarkable

improvements compared with the previous works on sliding mode based attitude control. First, the presented method can handle actuator uncertainties, including misalignments and faults, simultaneously. Second, the proposed strategy can asymptotically stabilize the satellite attitude with finite-time convergence. Although the developed method was found to guarantee good attitude control performance, it can also be enhanced further. For example, the implementation of the controller required exact knowledge of the satellite inertia. Extension of these results to situations handling an uncertain mass moment of inertia would be extremely beneficial.

## REFERENCES

[1] Z. Gao, C. Cecati, and S. X. Ding, "A survey of fault diagnosis and fault-tolerant techniques—Part I: Fault diagnosis with model-based and signal-based approaches," *IEEE Trans. Ind. Electron.*, vol. 62, no. 6, pp. 3757–3767, Jun. 2015.
[2] Z. Gao, C. Cecati, and S. X. Ding, "A survey of fault diagnosis and fault-tolerant techniques–Part II: Fault diagnosis with knowledge-based and hybrid/active approaches," *IEEE Trans. Ind. Electron.*, vol. 62, no. 6, pp. 3768–3774, Jun. 2015.
[3] Q. Meng, T. Zhang, X. Gao, and J.-Y. Song, "Adaptive sliding mode fault-tolerant control of the uncertain Stewart platform based on offline multibody dynamics," *IEEE/ASME Trans. Mechatronics*, vol. 19, no. 3, pp. 882–894, Jun. 2014.
[4] S. Yin, H. Gao, O. Kaynak, and J. Qiu, "Descriptor reduced-order sliding mode observers design for switched systems with sensor and actuator faults," *Automatica*, vol. 76, pp. 282–292, Feb. 2017.
[5] S. Yin, H. Yang, and O. Kaynak, "Sliding mode observer-based FTC for Markovian jump systems with actuator and sensor faults," *IEEE Trans. Autom. Control*, vol. 62, no. 7, pp. 3551–3558, Jul. 2017.
[6] Y. Cao and X. B. Chen, "An output-tracking-based discrete PID-sliding mode control for MIMO systems," *IEEE/ASME Trans. Mechatronics*, vol. 19, no. 4, pp. 1183–1194, Aug. 2014.
[7] S. Kurode, S. K. Spurgeon, B. Bandyopadhyay, and P. S. Gandhi, "Sliding mode control for slosh-free motion using a nonlinear sliding surface," *IEEE/ASME Trans. Mechatronics*, vol. 18, no. 2, pp. 714–724, Apr. 2013.
[8] A. Iyer and S. N. Singh, "Variable structure slewing control and vibration damping of flexible spacecraft," *Acta Astron.*, vol. 25, pp. 1–9, Jan. 1991.
[9] Y.-P. Chen and S.-C. Lo, "Sliding-mode controller design for spacecraft attitude tracking maneuvers," *IEEE Trans. Aerosp. Electron. Syst.*, vol. 29, no. 4, pp. 1328–1333, Oct. 1993.
[10] S.-C. Lo and Y. P. Chen, "Smooth sliding-mode control for spacecraft attitude tracking maneuvers," *J. Guid., Control, Dyn.*, vol. 18, no. 6, pp. 1345–1349, Nov./Dec. 1995.
[11] A. Taheri, M. A. Shoorehdeli, H. Bahrami, and M. H. Fatehi, "Implementation and control of X–Y pedestal using dual-drive technique and feedback error learning for leo satellite tracking," *IEEE Trans. Control Syst. Technol.*, vol. 22, no. 4, pp. 1646–1657, Jul. 2014.
[12] X. Zhao, H. Yang, H. R. Karimi, and Y. Zhu, "Adaptive neural control of MIMO nonstrict-feedback nonlinear systems with time delay," *IEEE Trans. Cybern.*, vol. 46, no. 6, pp. 1337–1349, Jun. 2016.
[13] X. Zhao, P. Shi, and X. Zheng, "Fuzzy adaptive control design and discretization for a class of nonlinear uncertain systems," *IEEE Trans. Cybern.*, vol. 46, no. 6, pp. 1476–1483, Jun. 2015.
[14] C. Pukdeboon, A. S. I. Zinober, and M.-W. L. Thein, "Quasi-continuous higher order sliding-mode controllers for spacecraft-attitude-tracking maneuvers," *IEEE Trans. Ind. Electron.*, vol. 57, no. 4, pp. 1436–1444, Apr. 2010.
[15] Z. Zhu, Y. Xia, and M. Fu, "Adaptive sliding mode control for attitude stabilization with actuator saturation," *IEEE Trans. Ind. Electron.*, vol. 58, no. 10, pp. 4898–4907, Oct. 2011.
[16] Z. Gao, X. Liu, and M. Z. Q. Chen, "Unknown input observer-based robust fault estimation for systems corrupted by partially decoupled disturbances," *IEEE Trans. Ind. Electron.*, vol. 63, no. 4, pp. 2537–2547, Apr. 2016.
[17] Z. Gao, "Fault estimation and fault-tolerant control for discrete-time dynamic systems," *IEEE Trans. Ind. Electron.*, vol. 62, no. 6, pp. 3874–3884, Jun. 2015.
[18] H. Hur and H.-S. Ahn, "Unknown input $H_\infty$ observer-based localization of a mobile robot with sensor failure," *IEEE/ASME Trans. Mechatronics*, vol. 19, no. 6, pp. 1830–1838, Dec. 2014.
[19] M. Tafazoli, "A study of on-orbit spacecraft failures," *Acta Astron.*, vol. 64, nos. 2–3, pp. 195–205, Jan./Feb. 2009.
[20] D. Bustan, S. K. H. Sani, and N. Pariz, "Adaptive fault-tolerant spacecraft attitude control design with transient response control," *IEEE/ASME Trans. Mechatronics*, vol. 19, no. 4, pp. 1404–1411, Aug. 2014.
[21] B. Xiao, Q. Hu, D. Wang, and E. K. Poh, "Attitude tracking control of rigid spacecraft with actuator misalignment and fault," *IEEE Trans. Control Syst. Technol.*, vol. 21, no. 6, pp. 2360–2366, Nov. 2013.
[22] S. Scarritt, "Nonlinear model reference adaptive control for satellite attitude tracking," in *Proc. AIAA Guid., Navigat. Control Conf. Exhib.*, Honolulu, Hawaii, 2008.
[23] R. Liu, G. Meng, B. Yang, C. Sun, and X. Chen, "Dislocated time series convolutional neural architecture: An intelligent fault diagnosis approach for electric machine," *IEEE Trans. Ind. Informat.*, vol. 13, no. 3, pp. 1310–1320, Jun. 2017, doi: 10.1109/TII.2016.2645238.
[24] S. Yin, J. Qiu, H. Gao, and O. Kaynak, "Fault detection for nonlinear process with deterministic disturbances: A just-in-time learning based data driven method," *IEEE Trans. Cybern.*, to be published, doi: 10.1109/TCYB.2016.2574754.
[25] G. He and Z. Geng, "Finite-time stabilization of a comb-drive electrostatic microactuator," *IEEE/ASME Trans. Mechatronics*, vol. 17, no. 1, pp. 107–115, Feb. 2012.
[26] B. Xiao, Q. Hu, and Y. Zhang, "Finite-time attitude tracking of spacecraft with fault-tolerant capability," *IEEE Trans. Control Syst. Technol.*, vol. 23, no. 4, pp. 1338–1350, Jul. 2015.
[27] E. Jin and Z. Sun, "Robust controllers design with finite time convergence for rigid spacecraft attitude tracking control," *Aerosp. Sci. Technol.*, vol. 12, pp. 324–330, Jun. 2008.
[28] S. Ding and S. Li, "Stabilization of the attitude of a rigid spacecraft with external disturbances using finite-time control techniques," *Aerosp. Sci. Technol.*, vol. 13, nos. 4–5, pp. 256–265, 2009.
[29] S. Wu, G. Radice, Y. Gao, and Z. Sun, "Quaternion-based finite time control for spacecraft attitude tracking," *Acta Astron.*, vol. 69, nos. 1–2, pp. 48–58, Jul./Aug. 2011.
[30] H. Du and S. Li, "Finite-time attitude stabilization for a spacecraft using homogeneous method," *J. Guid., Control, Dyn.*, vol. 35, no. 3, pp. 740–748, 2012.
[31] P. A. Servidia and R. S. S. Pena, "Practical stabilization in attitude thruster control," *IEEE Trans. Aerosp. Electron. Syst.*, vol. 41, no. 2, pp. 584–598, Apr. 2005.
[32] J. L. Crassidis and F. L. Markley, "Sliding mode control using modified Rodrigues parameters," *J. Guid., Control, Dyn.*, vol. 19, pp. 1381–1383, Nov./Dec. 1996.
[33] H. Schaub, M. R. Akella, and J. L. Junkins, "Adaptive control of nonlinear attitude motions realizing linear closed loop dynamics," *J. Guid., Control, Dyn.*, vol. 24, pp. 95–100, Jan./Feb. 2001.
[34] M. J. Sidi, *Spacecraft Dynamics and Control*. Cambridge, U.K.: Cambridge Univ. Press, 1997.
[35] A. Valdes and K. Khorasani, "A pulsed plasma thruster fault detection and isolation strategy for formation flying of satellites," *Appl. Soft Comput.*, vol. 10, pp. 746–758, Jun. 2010.
[36] H. K. Khalil, *Nonlinear Systems*, 3rd ed. Englewood Cliffs, NJ, USA: Prentice-Hall, 2002.
[37] I. Haskara, "On sliding mode observers via equivalent control approach," *Int. J. Control*, vol. 71, pp. 1051–1067, 1998.
[38] C. J. Fallaha, M. Saad, H. Y. Kanaan, and K. Al-Haddad, "Sliding-mode robot control with exponential reaching law," *IEEE Trans. Ind. Electron.*, vol. 58, no. 2, pp. 600–610, Feb. 2011.
[39] S. P. Bhat and D. S. Bernstein, "Finite-time stability of continuous autonomous systems," *SIAM J. Control Optim.*, vol. 38, no. 3, pp. 751–766, 2000.

**A. AIHUA ZHANG** received the bachelor's degree from the Jinzhou Teacher's College in 2000, the master's degree from Bohai University in 2008, and the Ph.D. degree from the Harbin Institute of Technology in 2014. She is currently a Professor with Bohai University. Her current research interests include fault diagnosis, fault tolerance, and attitude control of satellites.

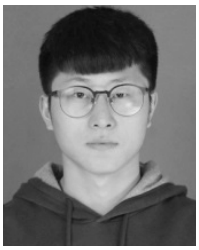

**B. CHENGCONG LV** received the bachelor's degree from the College of Engineering, Bohai University, in 2017, where he is currently pursuing the master's degree. His current research interests include fault diagnosis and fault tolerance.

**C. ZHIQIANG ZHANG** received the bachelor's degree from the Jinzhou Teacher's College in 2000 and the master's degree from the Dalian University of Technology in 2008. He is currently an Associate Professor with Bohai University. His current research interests include machine learning and pattern recognition.

**D. ZHIYONG SHE** received the bachelor's, master's, and Ph.D. degrees from the Harbin Institute of Technology, in 2004, 2006, and 2010, respectively. He is currently a Professor with Bohai University. His current research interests include fault diagnosis, fault tolerance, and attitude control of satellites.